

not use completely effective information to reveal individual differences. Meanwhile, drug molecules are usually composed of complex structures and multiple interacting attributes. Traditional drug molecule relationship extraction methods cannot capture complex patterns and interactions in a large amount of drug data [8], which limits the understanding of drug features and leads to the accuracy of model predictions is poor.

We propose a graph contrastive learning method with multi-omics for cancer drug response prediction (GCLM-CDR) to address the existing issues. Firstly, we constructed a multi-omics drug feature representation module to extract multi-omics and drug molecule features. This can fully capture the differences and correlations between multi-omics features, as well as better capture the correlation relationships between nodes in the drug molecular graphs. Secondly, we constructed a graph contrastive learning module to simultaneously capture and learn local structural information of multi-omics and drug molecules, as well as richer global information. It provides a more effective node feature embedding for drug response prediction and enhances the generalization ability of the model. Finally, we use a function to calculate the probability of predicting sensitive reactions between multi-omics and drugs. Compared with existing research methods, our model achieved better performance on both GDSC and CCLE datasets. The genomics of drug sensitivity in cancer (GDSC) [9] and cancer cell line encyclopedia (CCLE) [10] are two public databases established to store and share information related to cancer cell lines, providing researchers with richer resources to help them study the sensitivity and resistance of cancer cells to different drugs. By analyzing this data, researchers can better predict drug efficacy and develop personalized treatment strategies to improve the effectiveness of cancer treatment.

II. METHODS

As shown in Fig. 1, the framework of GCLM-CDR mainly includes three modules: (1) multi-omics drug feature representation module, (2) graph contrastive learning module, (3) cancer drug response prediction module.

A. Multi-omics drug feature representation module

In this module, we extract multi-omics data features through Deep Neural Networks (DNN). Then, multi-omics interaction is conducted to capture the differences between different omics, enhancing the complementarity and synergy between multi-omics features. Meanwhile, Graph Attention Network (GAT) is used to extract drug information with different complex structures, obtaining a more holistic representation of drug characteristics and enhancing the feature expression ability of drug molecules.

a) Multi-omics representation: firstly, we input three types of omics data (i.e. a genomic feature vector M_G , an epigenomic feature vector M_E and a transcriptomic feature vector M_N) into the deep neural network, and automatically learn the feature representation in the data through the hierarchical structure of the deep neural network, thereby learning a richer Multi-omics feature representation. We concatenate the

three omics data learned by DNN layers pairwise, and then conduct multi-omics interaction to strengthen the connection between the three omics. In order to discover the correlation and common characteristics between the three types of omics, we constructed a multi-omics Neighborhood Interaction (NI) layer, see (1):

$$M_j = M_a \odot M_b, j \in \{1, 2, 3\}; a, b \in \{G, E, N\} \text{ and } a \neq b \quad (1)$$

where \odot represents for element-wise dot product of multi-omics features.

In the NI layer, one type of omics data node element-wise dot product with two other neighboring omics data nodes. This process is applied to all three types of omics data to identify similarities and correlations between different omics data, thereby extracting more comprehensive information. Finally, the integrated omics data are consolidated into a whole, creating a comprehensive multi-omics feature representation denoted as M_C :

$$M_C = M_1 || M_2 || M_3 \quad (2)$$

where $||$ represents concatenation of M_1 , M_2 , and M_3 , connecting the interacted omics data into a whole.

By interacting and integrating three types of omics data, potential biological interconnections can be uncovered, offering insights for subsequent clinical analysis and interpretation.

b) Drug representation: drug molecules are composed of complex structures and multiple interacting attributes. Understanding the relationship between drug molecules is important for predicting drug effects. We represent drug smiles compiled into drug molecular graphs. We denote graph $G_D = (X_D, A_D)$. $X_D \in R^{N_D \times F_D}$ is a matrix that stores the attribute vectors of all drug atoms ($F_D=75$) and an adjacency matrix $A_D \in R^{N_D \times N_D}$ representing the keys, where N_D is the number of atoms in the drug molecule diagram D .

We use Graph Attention Networks (GAT) [11] to extract drug molecule graph features. GAT use the attention mechanism to dynamically calculate the relationship weights between nodes, so it can effectively capture the internal structural information of drug molecule graphs and the interaction between molecules. In order to obtain the weight of each neighboring node for all nodes, we train a shared weight matrix M . Map the representations of node α and node β using M respectively, use feedforward neural network \vec{A}^T to map the concatenated vectors onto real numbers, and activate them through LeakyReLU. After normalization, obtain the final attention coefficient $a_{\alpha\beta}$ as (4):

$$e_{\alpha\beta} = \text{LeakyReLU} \left(\vec{A}^T \left[M\vec{h}_\alpha || M\vec{h}_\beta \right] \right) \quad (3)$$

$$a_{\alpha\beta} = \text{softmax}_{\beta \in N_\alpha} e_{\alpha\beta} \frac{\exp(e_{\alpha\beta})}{\sum_{k \in N_\alpha} \exp(e_{\alpha k})} \quad (4)$$

Utilizing the derived attention weights, the neighboring nodes are aggregated with weighted importance. Then we obtained the output features of the nodes α as:

$$h'_\alpha = \sigma \left(\sum_{\beta \in N_\alpha} a_{\alpha\beta} W \vec{h}_\beta \right) \quad (5)$$

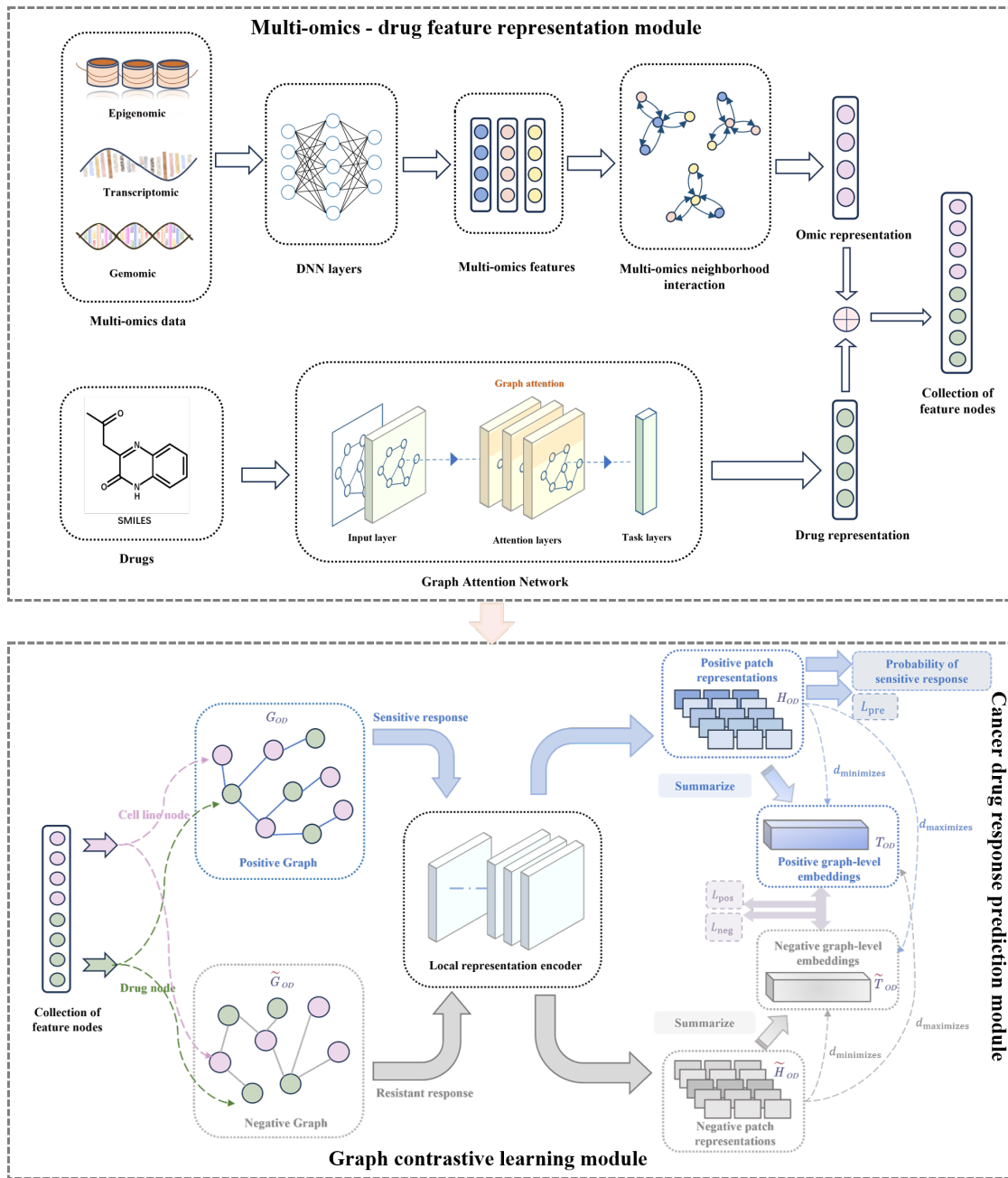


Fig. 1. Overview of GCLM-CDR framework.

Finally, we use a Global Maximum Pooling (GMP) layer to integrate the global representation of the extracted drug molecule graph, and the summarized drug feature representations nodes are used as effective inputs for subsequent modules.

B. Graph contrastive learning module

In recent years, contrastive learning has achieved a good performance in the field of graph learning [12]. Graph contrastive learning facilitates the acquisition of effective representations for drug molecular graphs, enhancing the model's ability to capture similarities and disparities among drugs.

Inspired by Heterogeneous Deep Graph Infomax [13], we constructed a graph contrastive learning module. We designate sensitive responses as positive responses and insensitive responses as negative responses based on known cell-drug responses. Firstly, we use the multi-omics nodes and drug nodes that extracted by the multi-omics drug feature representation module as the node set of the drug molecular graphs. Then, we use the sensitive/insensitive reactions between multi-omics and drugs as the edge set to construct an undirected heterogeneous graph $G_{OD} = (V, E)$, where V represents the node set containing multi-omics O and drug D that do not intersect ($|V| = N_O + N_D$), $E \subset V \times V$ represents the edges set

representing multi-omics and drug sensitive reactions. We can also use node attributes and adjacency matrices to represent the constructed graph: $G_{OD} = (X_{OD}, A_{OD})$, $X_{OD} \in \mathbb{R}^{|\mathcal{V}| \times F}$ represents node attributes and $A_{OD} \in \{0, 1\}^{|\mathcal{V}| \times |\mathcal{V}|}$ represents the adjacency matrix (“1” represents sensitive and “0” represents insensitive). By processing, we obtained positive graphs G_{OD} and negative graphs \tilde{G}_{OD} . After that, we built a local representation encoder $\Omega_{OD}: (X_{OD}, A_{OD}) \rightarrow H_{OD} \in \mathbb{R}^{|\mathcal{V}| \times F}$ to process the graph. We input graphs into the encoder, and obtain positive patch representations H_{OD} and negative patch representations \tilde{H}_{OD} . Ω_{OD} is set to a k_{OD} -layer ($k_{OD} = 1$) GCN with the PReLU [14] function, and the embedding of node $x \in \mathcal{V}$ can be expressed as:

$$\vec{h}_x^{(k_{OD})} = PReLU^{(k_{OD})} \left(\sum_{y \in \mathcal{N}(x) \cup \{x\}} \frac{1}{\sqrt{q_x q_y}} \cdot \mathbf{w}_{OD}^{(k_{OD})} \cdot \vec{h}_x^{(k_{OD}-1)} \right) \quad (6)$$

Positive graph-level embeddings T_{OD} and negative graph-level embeddings \tilde{T}_{OD} are summarized by passing the resulting patch representations to an attentive readout function R : $T_{OD} = \sum_{x \in \mathcal{V}} a_x \cdot \vec{h}_x^{(k_{OD})}$, a_x indicates the attention score of node x :

$$a_x = \frac{\exp \left(f_a \left(\left[\vec{h}_x^{(0)} \parallel \vec{h}_x^{(k_{OD})} \right] \right) \right)}{\sum_{x \in \mathcal{V}} \exp \left(f_a \left(\left[\vec{h}_x^{(0)} \parallel \vec{h}_x^{(k_{OD})} \right] \right) \right)} \quad (7)$$

where f_a is a fully connected layer used to map embeddings to real numbers. Similarly, $\tilde{T}_{OD} = R(\tilde{H}_{OD})$.

In order to help the model learn useful information from these complex structures, we express the goal of graph contrastive learning tasks as follows: (1) maximizing mutual information between positive graph-level embeddings and positive patch representations. (2) maximizing disagreements between positive patch representations and negative graph-level embeddings. And we define the loss function of the graph contrastive learning module as the following two parts:

$$\mathcal{L}_{pos} = -\frac{1}{2|\mathcal{V}|} \left(\sum_{x \in \mathcal{V}} \log D(\vec{h}_x, T) + \sum_{x \in \mathcal{V}} \log \left(1 - D(\vec{h}_x, \tilde{T}) \right) \right) \quad (8)$$

$$\mathcal{L}_{neg} = -\frac{1}{2|\mathcal{V}|} \left(\sum_{x \in \mathcal{V}} \log D(\vec{h}_x, \tilde{T}) + \sum_{x \in \mathcal{V}} \log \left(1 - D(\vec{h}_x, T) \right) \right) \quad (9)$$

where $D(\cdot, \cdot)$ is a discriminator evaluates similarities between the patch representations and the graph-level embedding. The discriminator constructed by a function $\sigma(\vec{h}^T W T)$, W is a learnable scoring matrix, σ is a logistic sigmoid nonlinearity.

C. Cancer drug response prediction module

We extract the final embeddings of multi-omics and drugs from the positive patch representations, and activate them through linear transformation and sigmoid function. We represent $\vec{h}_O = H_{OD}[O, :]$ and $\vec{h}_D = H_{OD}[D, :]$ as the final embeddings of multi-omics node O and drug node D , respectively. Finally, we calculate the inner product between the \vec{h}_O and

\vec{h}_D through the function to predict the probability of sensitive reactions \hat{P}_{OD} :

$$\hat{P}_{OD} = \text{Sigmoid}(\vec{h}_O \vec{h}_D^T) \quad (10)$$

We define the loss function of the drug response prediction module as:

$$\mathcal{L}_{pre} = -\frac{1}{|Y|} \sum_{(O,D) \in Y} \left(P_{OD} \log \hat{P}_{OD} + (1 - P_{OD}) \log (1 - \hat{P}_{OD}) \right) \quad (11)$$

where Y is the training set of responses, P_{OD} is the label for the response between nodes O and D .

D. Optimization

In order to improve the predictive performance and reliability of the model, we combined (8), (9) and (11) to optimize the objective:

$$\mathcal{L} = (1 - \lambda - \mu) \mathcal{L}_{pre} + \lambda \mathcal{L}_{pos} + \mu \mathcal{L}_{neg} \quad (12)$$

where λ and μ are hyper-parameters that balance the contribution of graph contrastive learning task and the drug response prediction task. After setting hyper-parameter optimization validation on the GDSC dataset, the model achieved the best performance at 0.3, so we fixed the hyper-parameter λ and μ to 0.3.

III. EXPERIMENTS

A. Datasets

In this section, we will provide a brief overview of the dataset. Our dataset come from three resources: CCLE, GDSC and PubChem.

- CCLE contains a large number of molecular characteristics data of cancer cell lines. We downloaded three types of omics data (gene expression, genome mutation and DNA methylation) from the DeMap portal (<https://depmap.org/>). The specific processing method is similar to GraphCDR [6]. The final datas are: 34,673-dimensional genome feature vector, 808-dimensional epigenome feature vector, and 697-dimensional transcriptome feature vector.
- GDSC contains a large amount of data on drug sensitivity of various tumor cells. We mainly collected IC50 values as a measure of the response. We binarized the IC50 value based on the threshold in the existing report [15] as a criterion for judging whether the drug is sensitive to cells. After processing, we finally obtained a reaction dataset containing 222 drugs and 561 cell lines (including 88,981 resistant reactions and 11,591 sensitive reactions). Some IC50 values in this data are unknown/missing.
- PubChem is a chemical information database that provides SMILES strings for many drugs. We downloaded the required drug data and use the ConvMolFeaturizer method [16] from the DeepChem library to compile the drug SMILES string into the desired drug molecular diagram. Through processing, the attributes of drug atomic nodes are represented as 75-dimensional feature vectors.

B. Model evaluation

In this research, the GDSC dataset was employed as the main dataset for evaluating the performance of the GCLM-CDR. We consider drug-sensitive reactions as positive samples and drug-resistant reactions as negative samples. We divide the response data on GDSC dataset into the cross-validation sets and independent test sets respectively at a ratio of 9:1, and ensure that there is no overlap between these two parts of data. Some of the experimental settings are as follows:

- Cross-validation: we randomly divide the drug responses dataset into five equal parts and employ 5-fold cross-validation (5-CV). In each iteration, we train the model on four parts of the data (the train set) and evaluate its performance on the remaining part (the test set).
- Independent test: we validate the performance of GCLM-CDR through independent testing. Except for the GDSC dataset, we also additionally carried out an independent test utilizing the CCLE dataset.
- Evaluation metrics: Area Under the Curve (AUC) provide a general measure of model effectiveness, and Area Under the Precision-Recall Curve (AUPR) provide insight into the model’s performance. AUC and AUPR are two performance metrics used to evaluate the accuracy of classification models.

C. Experimental comparison

We choose the following baselines to conduct the comprehensive evaluation of our model:

- GraphCDR [6] constructs a graph data representation of multi-omics data and drug molecular structure, which combined graph neural network and contrastive learning to learn more discriminative node representations, and finally to predict cancer drug response.
- DeepCDR [17] converts multi-omics data and drug molecular structures into graph data representation, and then uses a hybrid graph convolutional network to learn these graph data. Finally, the learned feature representations are input into a prediction model to predict drug response to different cancer cell lines.
- DeepDSC [8] extracts genomic features of cancer cell lines from gene expression data using a stacked depth autoencoder, and then combined the chemical information of the compounds with the genomic features to predict the IC50 value of the drug.

The results on the GDSC and CCLE datasets are shown in Table I and Table II.

a) *Test results on the GDSC dataset:* we adopted the 5-fold cross-validation (5-CV) on GDSC dataset, and compared our model with other baselines. As shown in Table I, our model outperforms other baselines, achieving the highest AUC score 0.8534 and AUPR score 0.5327.

b) *Test results on the CCLE dataset:* we also conducted independent tests on the CCLE dataset, which allowed us to further evaluate the model’s performance on unfamiliar data and evaluate the model’s performance more objectively. As

TABLE I
THE RESULTS ON GDSC DATASET

Method	AUC	AUPR
DeepDSC	0.7592	0.4236
DeepCDR	0.8221	0.4622
GraphCDR	0.8451	0.5210
GCLM-CDR	0.8534	0.5327

shown in Table II, our experimental results on the CCLE dataset are also better than other baselines, achieving the highest AUC score 0.9599 and AUPR score 0.8715.

TABLE II
THE RESULTS ON CCLE DATASET

Method	AUC	AUPR
DeepDSC	0.9305	0.8363
DeepCDR	0.9420	0.8225
GraphCDR	0.9467	0.8594
GCLM-CDR	0.9599	0.8715

Compared with other baselines, the results indicate that our model has achieved the highest performance in predicting multi-omics drug responses in cancer, indicating that our model has high generalization ability.

D. Ablation study

Our study included multiple modules to predict drug response. In order to further investigate the impact and importance of each component on the prediction task, we designed the following ablation experiments on GDSC dataset to verify. Our settings are shown in Table III:

TABLE III
RESULTS OF ABLATION STUDY

Method	AUC	AUPR
w/o Genomic mutation	0.8473	0.5212
w/o Gene expression	0.8498	0.5271
w/o DNA methylation	0.8506	0.5293
w/o Multi-omics interaction	0.8178	0.4610
w/o CL task	0.8294	0.4901
w/o GAT	0.8053	0.4315
Full model	0.8534	0.5327

In Table III, “w/o Genomic mutation” means our model has no genetic mutation data, “w/o Gene expression” means our model has no gene expression data, “w/o DNA methylation” means our model has no DNA methylation data, “w/o Multi-omics interaction” means our model removes interactions with multi-omics data, “w/o CL task” means our model has deleted the contrastive learning task in the module, “w/o GAT” means our model not use GAT to extract drug molecule graphs.

We conducted ablation experiments using 5-CV on the GDSC dataset. Based on the results, when any one of the three omics data is deleted, the AUC and AUPR scores will

be lower than the original model, indicating that all the three types of omics data have a certain impact and contribution to drug response prediction. After removing the GAT, the AUC and AUPR scores also decrease, indicating that GAT can selectively aggregate node information from drug molecular graphs through attention mechanisms, thereby improving prediction accuracy. When we delete the multi-omics data interaction module, the AUC and AUPR scores will decrease. This indicates that we not only need to use multi-omics data for prediction, but also need to pay attention to the connections between different omics. We should enhance the complementarity and synergy between multi-omics features. When we removed the contrastive learning task, the experimental results decreased, indicating that using the contrastive learning task can make a certain contribution to the drug response prediction task.

IV. CONCLUSION

This paper proposes a model GCLM-CDR, which can capture the differences and correlations between different multi-omics and effectively extract complex structural patterns of drug molecules. The graph contrastive learning module constructed in GCLM-CDR can further enhance the feature representation after the fusion of multi-omics and drug molecules. By focusing on increasing the match between positive samples while decreasing the match between negative ones, it helps the model learn to identify features that are widely applicable, enhancing its capability to forecast drug reactions. The empirical outcomes indicate that the GCLM-CDR outperforms current methodologies on both the GDSC and CCLE datasets.

In the future, we plan to develop novel approaches to data augmentation, designed to expand the training dataset and strengthen the model's capacity to generalize.

ACKNOWLEDGMENT

Thanks to the projects with No. 62162023 and No. KYQD(ZR)-21079 for support.

REFERENCES

- [1] W. Cao, H.-D. Chen, Y.-W. Yu, N. Li, and W.-Q. Chen, "Changing profiles of cancer burden worldwide and in china: a secondary analysis of the global cancer statistics 2020," *Chinese Medical Journal*, vol. 134, no. 07, pp. 783–791, 2021.
- [2] H. Zou and T. Hastie, "Regularization and variable selection via the elastic net," *Journal of the Royal Statistical Society Series B: Statistical Methodology*, vol. 67, no. 2, pp. 301–320, 2005.
- [3] P. Geleher, N. Cox, and R. Huang, "Clinical drug response can be predicted using baseline gene expression levels and," *Vitro Drug Sensitivity Cell Lines. Genome Biol*, vol. 15, p. R47, 2014.
- [4] H. Sharifi-Noghabi, O. Zolotareva, C. C. Collins, and M. Ester, "Moli: multi-omics late integration with deep neural networks for drug response prediction," *Bioinformatics*, vol. 35, no. 14, pp. i501–i509, 2019.
- [5] Z. Zuo, P. Wang, X. Chen, L. Tian, H. Ge, and D. Qian, "Swnet: a deep learning model for drug response prediction from cancer genomic signatures and compound chemical structures," *BMC Bioinformatics*, vol. 22, pp. 1–16, 2021.
- [6] X. Liu, C. Song, F. Huang, H. Fu, W. Xiao, and W. Zhang, "Graphcdr: a graph neural network method with contrastive learning for cancer drug response prediction," *Briefings in Bioinformatics*, vol. 23, no. 1, p. bbab457, 2022.

- [7] Y. Li, Z. Guo, X. Gao, and G. Wang, "Mmcl-cdr: enhancing cancer drug response prediction with multi-omics and morphology images contrastive representation learning," *Bioinformatics*, vol. 39, no. 12, p. btad734, 2023.
- [8] M. Li, Y. Wang, R. Zheng, X. Shi, Y. Li, F.-X. Wu, and J. Wang, "Deepdsc: a deep learning method to predict drug sensitivity of cancer cell lines," *IEEE/ACM Transactions on Computational Biology and Bioinformatics*, vol. 18, no. 2, pp. 575–582, 2019.
- [9] W. Yang, J. Soares, P. Greninger, E. J. Edelman, H. Lightfoot, S. Forbes, N. Bindal, D. Beare, J. A. Smith, I. R. Thompson *et al.*, "Genomics of drug sensitivity in cancer (gdsc): a resource for therapeutic biomarker discovery in cancer cells," *Nucleic Acids Research*, vol. 41, no. D1, pp. D955–D961, 2012.
- [10] J. Barretina, G. Caponigro, N. Stransky, K. Venkatesan, A. A. Margolin, S. Kim, C. J. Wilson, J. Lehár, G. V. Kryukov, D. Sonkin *et al.*, "The cancer cell line encyclopedia enables predictive modelling of anticancer drug sensitivity," *Nature*, vol. 483, no. 7391, pp. 603–607, 2012.
- [11] P. Velickovic, G. Cucurull, A. Casanova, A. Romero, P. Lio, Y. Bengio *et al.*, "Graph attention networks," *Stat*, vol. 1050, no. 20, pp. 10–48 550, 2017.
- [12] S. Zhang and Q. Zhang, "Adcl: an adaptive dual contrastive learning framework based on mhgat and vae for cell type deconvolution in spatial transcriptomics," in *2023 IEEE International Conference on Bioinformatics and Biomedicine (BIBM)*. IEEE, 2023, pp. 355–358.
- [13] Y. Ren, B. Liu, C. Huang, P. Dai, L. Bo, and J. Zhang, "Heterogeneous deep graph infomax," *ArXiv*, 2019, <https://doi.org/10.48550/arXiv.1911.08538>.
- [14] K. He, X. Zhang, S. Ren, and J. Sun, "Delving deep into rectifiers: Surpassing human-level performance on imagenet classification," in *Proceedings of the IEEE International Conference on Computer Vision*, 2015, pp. 1026–1034.
- [15] F. Iorio, T. A. Knijnenburg, D. J. Vis, G. R. Bignell, M. P. Menden, M. Schubert, N. Aben, E. Gonçalves, S. Barthorpe, H. Lightfoot *et al.*, "A landscape of pharmacogenomic interactions in cancer," *Cell*, vol. 166, no. 3, pp. 740–754, 2016.
- [16] D. K. Duvenaud, D. Maclaurin, J. Iparraguirre, R. Bombarell, T. Hirzel, A. Aspuru-Guzik, and R. P. Adams, "Convolutional networks on graphs for learning molecular fingerprints," *Advances in Neural Information Processing Systems*, vol. 28, 2015.
- [17] Q. Liu, Z. Hu, R. Jiang, and M. Zhou, "Deepcdr: a hybrid graph convolutional network for predicting cancer drug response," *Bioinformatics*, vol. 36, pp. i911–i918, 2020.